International Journal of Control, Automation, and Systems 20(7) (2022) 2159-2168
http://dx.doi.org/10.1007/s12555-021-0206-x

ISSN:1598-6446 eISSN:2005-4092
http://www.springer.com/12555

A Simple Frequency-domain Tuning Method of Fractional-order PID Controllers for Fractional-order Delay Systems

Xu Li* and **Lifu Gao**

Abstract: The fractional-order proportional-integral-derivative (FOPID) controller is an improvement over the traditional PID controller. However, most existing methods of FOPID controller design are complex and not suitable for practical application. This paper presents a simple and efficient design method of FOPID controllers for fractional-order controlled plants with time delays. The method is based on four frequency-domain specifications—namely, gain crossover frequency, phase margin, phase crossover frequency and gain margin. The implicit nonlinear equations related to the controller parameters are formulated using these specifications. To simplify the mathematical calculation, the explicit equations of the controller parameters are analytically derived. Then, the FOPID controller parameters can be adjusted in a graphical manner. Two fractional-order plus time-delay plants are considered as simulation examples. The results show that the design requirements are successfully met and superior control performance is obtained via the proposed tuning method.

Keywords: FOPID controller, fractional-order systems, frequency-domain specifications, time delay.

1. INTRODUCTION

In recent decades, fractional calculus has gained considerable traction as an important mathematical approach. It is an important tool for the profound depiction of physical processes in the real world and can be used in many fields of study, such as thermal diffusion [1], chaotic systems [2], viscoelasticity [3], signal processing [4], mechatronic systems [5], and neural networks [6]. The fractional-order derivative, for example, has been used to manage a hydraulic servo system with strong historical dependency and mechanical inertia [7]. Fractional calculus has also been widely applied in system modeling and controller design research [8–11].

Many inherently complex industrial processes can be described as high-order models. In practice, to minimize the cost of system analysis and design, simplified models are typically used to estimate these processes. The most widely used templates are the first-order plus time delay (FOPTD) and the second-order plus time delay (SOPTD) versions. Nevertheless, the FOPTD and SOPTD models cannot delicately characterize the dynamic behavior of complex systems. For example, underdamped dynamical processes cannot be well modeled by FOPTD transfer functions [12]. In an increasing number of studies, fractional-order models have been considered to improve modeling accuracy [13–17].

Recently, most industrial processes have been regulated by PID controllers. Inspired by the principle of fractional calculus, PID controllers are modified into a new form of FOPID to boost the control efficiency. In terms of robustness and closed-loop response performance, FOPID controllers outperform PID controllers [18,19]. Because of the additional two adjustable orders, tuning the parameters of FOPID controllers is not an easy task, especially for fractional-order systems with time delays. The current research on this subject can be divided into time-domain methods, frequency-domain methods and synthesis methods. Time-domain methods use optimization algorithms, such as particle swarm optimization [20], differential evolution algorithms [21], and radial basis function neural networks [22], to tune the FOPID parameters; however, these optimization methods are time consuming to apply, and the resulting controllers may lack robustness. Considering these factors, many researchers prefer frequency-domain approaches. In [23–26], the controller parameters were determined by a series of nonlinear equations related to gain crossover frequency, phase margin, sensitivity functions and the "flat phase" criterion, but the solution was difficult to obtain. In [27,28], FOPID controllers were designed based on Bode's ideal transfer function. The design processes include complex calculations, such as data

Manuscript received March 10, 2021; revised August 3, 2021; accepted September 18, 2021. Recommended by Associate Editor Jun Cheng under the direction of Editor Yoshito Ohta.

Xu Li and Lifu Gao are with the Institute of Intelligent Machines, Hefei Institutes of Physical Science, Chinese Academy of Sciences, No. 350 Shushan Road, Hefei 230031, China (e-mails: lx_tyq@163.com, lifugao@iim.ac.cn). Xu Li is also with the University of Science and Technology of China, No. 96 JinZhai Road Baohe District, Hefei 230026, China.
* Corresponding author.

fitting.

The complex design and implementation processes make FOPID controllers unattractive for industrial applications. As special cases of FOPID controllers, fractional-order proportional-integral (FOPI) and fractional-order proportional-derivative (FOPD) controllers appear to be more acceptable to engineers due to their simple structure and easy tuning [29–33]. Although FOPI and FOPD controllers perform better than PID controllers, they are inferior to FOPID controllers. Some researchers have made valuable attempts and explorations to preserve the FOPID structure and reduce the tuning difficulty. In [34], the number of adjustable controller parameters was reduced from five to three by establishing a proportional relationship between them. The tuning procedure is complicated and includes data fitting and optimization. Reference [35] presented a simple FOPID tuning method for integer-order plants that still must solve a system of implicit nonlinear equations.

In this paper, a novel and simple FOPID controller design method is proposed for fractional-order systems with time delays. To the best of our knowledge, most previous studies concentrate on the gain crossover frequency and phase margin but neglect the phase crossover frequency and gain margin. One advantage of our strategy is that the four frequency-domain specifications are utilized simultaneously to achieve more comprehensive stability and robustness of the control system. Furthermore, the commonly used "flat phase" criterion, which often entails considerable computational difficulty, is abandoned. Flattening the phase curve is helpful to enhance the robustness of the system to gain variation. However, the gain margin presented on the magnitude curve is also important for the robustness of the system. In contrast, the proposed method provides a clear framework to shape the Bode plots of open-loop systems. Thus, the controller can be designed in a more comprehensive manner. Another innovation of this method is that the tuning process does not depend on a large number of implicit nonlinear equations. Solving nonlinear equations is laborious and tedious. To avoid complicated calculations and simplify the design process, the four implicit nonlinear equations determined by the frequency-domain specifications are skillfully converted into a single equation, which can be easily solved by following the graphical approach. After solving this equation, the parameters of the FOPID controller can be obtained immediately.

This paper is organized as follows: In Section 2, fractional-order control systems, FOPID controllers and frequency-domain specifications are introduced. Section 3 presents the novel design method for the FOPID controller. Two examples are illustrated in Section 4. Finally, conclusions are discussed in Section 5.

2. PRELIMINARIES

2.1. Fundamentals of fractional-order calculus

Fractional-order calculus is a generalization of traditional integer-order calculus, where the order of derivatives and integrals can be a real or complex number. Multiple mathematical explanations of fractional-order calculus exist, such as the Riemann-Liouville definition, Grunwald-Letnikov definition and Caputo definition [36]. The widely used Riemann-Liouville definition is shown as follows.

Definition 1: For an n-order differentiable function $f(t)$, the Riemann-Liouville derivative of order p is defined as

$$ {}_{t_0}D_t^p f(t) = \frac{1}{\Gamma(n-p)} \frac{d^n}{dt^n} \int_0^t (t-\tau)^{n-p-1} f(\tau) d\tau, \quad (1) $$

where n is a positive integer, $n-1 < p < n$, and $\Gamma()$ represents the gamma function.

Definition 2: For an integrable function $f(t)$, the Riemann-Liouville integral of order q is defined as

$$ {}_0J_t^q = \frac{1}{\Gamma(q)} \int_0^t (t-\tau)^{q-1} f(\tau) d\tau, \quad (2) $$

where q is a positive real number.

Under zero initial conditions, the Laplace transform of the Riemann-Liouville derivative and integral can be expressed as

$$ L\left[{}_0D_t^p f(t)\right] = s^p F(s), \quad (3) $$

and

$$ L\left[{}_0J_t^q f(t)\right] = s^{-q} F(s), \quad (4) $$

respectively.

2.2. The considered fractional-order plants and the FOPID controller

In this study, a fractional-order controlled plant with a wide application scope is discussed. Its transfer function is as follows:

$$ P(s) = \frac{K}{T_n s^{\gamma_n} + T_{n-1} s^{\gamma_{n-1}} + \cdots + T_0} e^{-Ls}, \quad (5) $$

where K is the plant gain; L is the time delay; T_i ($i \in \{1,$ 2, ..., $n\}$) is the coefficient; and γ_i denotes a positive real number satisfying $\gamma_{i+1} > \gamma_i$. This plant has been successfully used in the modeling of practical processes.

The general structure of a FOPID controller is as follows:

$$ C_{FOPID}(s) = k_p + \frac{k_i}{s^\lambda} + k_d s^\mu, \quad (6) $$

where k_p, k_i, and k_d denote the gains of the proportion, integration and differentiation components, respectively,

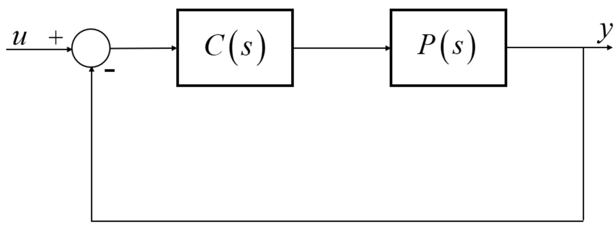

Fig. 1. Closed-loop control system.

and the fractional orders λ and μ satisfy $\lambda \in (0, 2)$ and $\mu \in (0, 2)$.

To simplify the design procedure, we set $\lambda = \mu = \nu$ and $\nu \in (0, 2)$. Thus, FOPID controller (6) can be modified to

$$C(s) = k_p + \frac{k_i}{s^{\nu}} + k_d s^{\nu}. \tag{7}$$

Due to the reduction in the number of adjustable parameters, the FOPID structure (6) is more compact, which greatly facilitates the design and implementation of the controller. In fact, the integral and derivative terms compensate for each other under the condition $\lambda = \mu$, which is beneficial to stability [35]. The fractional-order integral term eliminates the steady-state error while decreasing the relative stability due to the introduced $\lambda\pi/2$ phase lag. The fractional-order derivative action, moreover, has the benefit of increasing relative stability due to the introduced $\mu\pi/2$ phase lead but at the expense of increasing sensitivity to high-frequency noise. As a result of allowing $\lambda = \mu$, the increase in relative stability caused by the derivative compensates for the decrease in relative stability caused by the integral.

2.3. Frequency-domain specifications

Consider the closed-loop control system depicted in Fig. 1. The open-loop transfer function can be given as

$$G(s) = P(s)C(s). \tag{8}$$

To obtain better control performance, the gain crossover frequency, phase crossover frequency, gain margin and phase margin are utilized simultaneously in the proposed design procedure. These four frequency-domain characteristics provide a basic framework for the Bode plots of open-loop systems. As illustrated in Fig. 2, the gain crossover frequency ω_{gc} represents the frequency point at which the magnitude curve intersects the 0 dB line, while the phase margin ϕ_m is the difference between the phase curve and the -180° line at ω_{gc}. The phase crossover frequency ω_{pc} denotes the frequency point at which the phase curve crosses the -180° line, while the gain margin A denotes the difference between the magnitude curve and the 0 dB line at ω_{pc}. By adjusting these frequency-domain specifications, curves of different magnitudes and phases can be obtained.

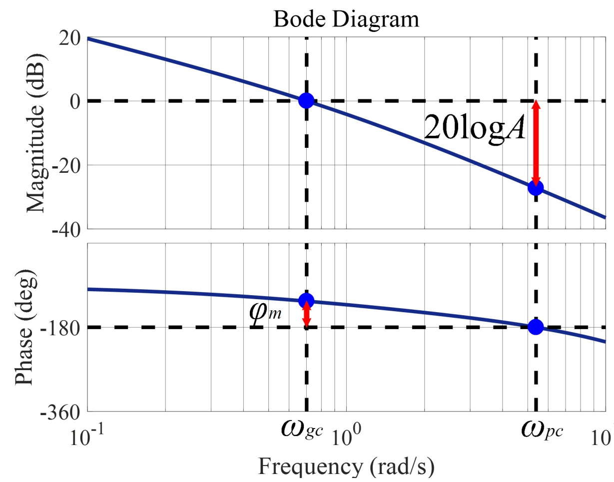

Fig. 2. Illustration of frequency-domain specifications.

Because there are four unknown parameters, the FOPID controller (7) can be uniquely determined under the four specifications. The corresponding equations are as follows:

(i) At ω_{gc}, we have

$$|G(j\omega_{gc})| = 1, \tag{9}$$
$$\angle G(j\omega_{gc}) = -\pi + \phi_m. \tag{10}$$

(ii) At ω_{pc}, we have

$$|G(j\omega_{pc})| = 1/A, \tag{11}$$
$$\angle G(j\omega_{pc}) = -\pi. \tag{12}$$

The FOPID controller parameters can be obtained by solving (9)-(12); however, the above four equations are nonlinear and implicit, which entails considerable difficulty in the calculation. Moreover, whether this set of equations can be solved under the given frequency-domain specifications is difficult to determine. A new design technique to overcome the abovementioned problems is presented in the following section.

3. THE PROPOSED DESIGN METHOD

3.1. Frequency response of the control system

By replacing s with $j\omega$ in (5), the frequency response of the fractional-order controlled plant can be expressed as

$$P(j\omega) = \frac{Ke^{-jL\omega}}{D_1(\omega) + jD_2(\omega)} = \frac{Ke^{-j(L\omega+\theta(\omega))}}{D(\omega)}, \tag{13}$$

where

$$D_1(\omega) = \sum_{i=1}^{n} T_i \omega^{\gamma_i} \cos\left(\frac{\pi}{2}\gamma_i\right) + T_0,$$

$$D_2(\omega) = \sum_{i=1}^{n} T_i \omega^{\gamma_i} \sin\left(\frac{\pi}{2}\gamma_i\right),$$

$$D(\omega)=\sqrt{D_1^2(\omega)+D_2^2(\omega)},$$
$$\theta(\omega)=\angle\left(D_1(\omega)+jD_2(\omega)\right).$$

The FOPID controller (7) can also be expressed as

$$C(j\omega)=C_1(\omega)+jC_2(\omega), \tag{14}$$

where

$$C_1(\omega)=k_p+k_i\omega^{-v}\cos\frac{\pi}{2}v+k_d\omega^{v}\cos\frac{\pi}{2}v,$$
$$C_2(\omega)=-k_i\omega^{-v}\sin\frac{\pi}{2}v+k_d\omega^{v}\sin\frac{\pi}{2}v.$$

Then, the open-loop transfer function $G(j\omega)$ is written as

$$G(j\omega)=\frac{C(j\omega)}{D(\omega)}Ke^{-j(L\omega+\theta(\omega))}. \tag{15}$$

Based on the expressions of $P(j\omega)$, $C(j\omega)$ and $G(j\omega)$, several theorems can be defined to compute the FOPID parameters.

3.2. Main results

The following theorems are proposed to solve (9)-(12).

Theorem 1: For the open-loop system (15), the FOPID parameters k_p and k_i that ensure constraints (9) and (10) can be determined by the following equations

$$k_p=-\frac{k_d\omega_{gc}^{v}\sin(\pi v)}{\sin\frac{\pi}{2}v}-\frac{D(\omega_{gc})\sin\left(\frac{\pi}{2}v+\theta_1\right)}{K\sin\frac{\pi}{2}v}, \tag{16}$$

$$k_i=k_d\omega_{gc}^{2v}+\omega_{gc}^{v}\frac{D(\omega_{gc})\sin\theta_1}{K\sin\frac{\pi}{2}v}, \tag{17}$$

where $\theta_1=\phi_m+L\omega_{gc}+\theta(\omega_{gc})$.

Proof: By substituting (16) and (17) into (14), $C(j\omega_{gc})$ can be calculated as follows:

$$\begin{aligned}C(j\omega_{gc})&=k_d\omega_{gc}^{v}\left(-\frac{\sin\pi v}{\sin\frac{\pi}{2}v}+e^{-j\frac{\pi}{2}v}+e^{j\frac{\pi}{2}v}\right)\\&\quad+D(\omega_{gc})\frac{e^{-j\frac{\pi}{2}v}\sin\theta_1-\sin\left(\frac{\pi}{2}v+\theta_1\right)}{K\sin\left(\frac{\pi}{2}v\right)}\\&=\frac{D(\omega_{gc})}{K}e^{j(-\pi+\theta_1)}.\end{aligned} \tag{18}$$

Combining (15) and (18) yields

$$|G(j\omega_{gc})|=\left|\frac{D(\omega_{gc})}{K}\right|\times\left|\frac{K}{D(\omega_{gc})}\right|=1, \tag{19}$$

$$\angle G(j\omega_{gc})=\angle e^{j(-\pi+\theta_1-L\omega_{gc}-\theta(\omega_{gc}))}=-\pi+\phi_m. \tag{20}$$

This completes the proof. □

Theorem 2: For the open-loop system (15), the FOPID parameters k_p and k_i that ensure constraints (11) and (12) can be determined by the following equations:

$$k_p=-\frac{k_d\omega_{pc}^{v}\sin(\pi v)}{\sin\frac{\pi}{2}v}-\frac{D(\omega_{pc})\sin\left(\frac{\pi}{2}v+\theta_2\right)}{AK\sin\frac{\pi}{2}v}, \tag{21}$$

$$k_i=k_d\omega_{pc}^{2v}+\omega_{pc}^{v}\frac{D(\omega_{pc})\sin\theta_2}{AK\sin\frac{\pi}{2}v}, \tag{22}$$

where $\theta_2=L\omega_{pc}+\theta(\omega_{pc})$.

Proof: Similar to the proof of Theorem 1, we first calculate $C(j\omega_{pc})$ utilizing (21) and (22) such that

$$\begin{aligned}C(j\omega_{pc})&=k_d\omega_{pc}^{v}\left(-\frac{\sin\pi v}{\sin\frac{\pi}{2}v}+e^{-j\frac{\pi}{2}v}+e^{j\frac{\pi}{2}v}\right)\\&\quad+D(\omega_{pc})\frac{e^{-j\frac{\pi}{2}v}\sin\theta_2-\sin\left(\frac{\pi}{2}v+\theta_2\right)}{AK\sin\left(\frac{\pi}{2}v\right)}\\&=\frac{D(\omega_{pc})}{AK}e^{j(-\pi+\theta_2)}.\end{aligned} \tag{23}$$

Then, we obtain

$$|G(j\omega_{pc})|=\left|\frac{D(\omega_{pc})}{AK}\right|\times\left|\frac{K}{D(\omega_{pc})}\right|=\frac{1}{A}, \tag{24}$$

$$\angle G(j\omega_{pc})=\angle e^{j(-\pi+\theta_2-L\omega_{pc}-\theta(\omega_{pc}))}=-\pi. \tag{25}$$

This completes the proof. □

Theorem 3: If the FOPID controller (7) satisfies constraints (9)-(12) for the given values of ω_{gc}, ω_{pc}, ϕ_m and A ($\omega_{gc}\neq\omega_{pc}$), then the following equation holds

$$AF_1(v)=F_2(v), \tag{26}$$

where

$$F_1(v)=D(\omega_{gc})\left(\sin\left(\frac{\pi}{2}v+\theta_1\right)-\omega_{gc}^{v}E(v)\sin\theta_1\right),$$
$$F_2(v)=D(\omega_{pc})\left(\sin\left(\frac{\pi}{2}v+\theta_2\right)-\omega_{pc}^{v}E(v)\sin\theta_2\right),$$
$$E(v)=2\frac{\omega_{pc}^{v}-\omega_{gc}^{v}}{\omega_{pc}^{2v}-\omega_{gc}^{2v}}\cos\left(\frac{\pi}{2}v\right).$$

Proof: From (16) and (21), we can obtain

$$\begin{aligned}&Kk_d\sin(\pi v)\\&=\frac{D(\omega_{gc})\sin\left(\frac{\pi}{2}v+\theta_1\right)}{\omega_{pc}^{v}-\omega_{gc}^{v}}-\frac{D(\omega_{pc})\sin\left(\frac{\pi}{2}v+\theta_2\right)}{A(\omega_{pc}^{v}-\omega_{gc}^{v})}.\end{aligned} \tag{27}$$

Similarly, it can be deduced from (17) and (22) that

$$\begin{aligned}&Kk_d\sin\left(\frac{\pi}{2}v\right)\\&=\frac{\omega_{gc}^{v}D(\omega_{gc})\sin\theta_1}{\omega_{pc}^{2v}-\omega_{gc}^{2v}}-\frac{\omega_{pc}^{v}D(\omega_{pc})\sin\theta_2}{A(\omega_{pc}^{2v}-\omega_{gc}^{2v})}.\end{aligned} \tag{28}$$

By combining (27) and (28), controller parameter k_d is eliminated, and (26) can be obtained. This completes the proof. □

Remark 1: The original nonlinear equations (9)-(12) are simplified substantially by utilizing the above three theorems. After specifying the values for ω_{gc}, ω_{pc}, ϕ_m and A, v can be obtained by solving (26). Then, k_d, k_p and k_i

can be computed directly via (28), (16) and (17), respectively. Clearly, only one implicit nonlinear equation must be solved in the tuning process.

Remark 2: Note that (26) is implicit for v but explicit for A, and the graphical approach should be a suitable candidate for addressing this equation. For fixed values of ω_{gc}, ω_{pc}, and ϕ_m, the value of A can be divided into the following three cases.

Case 1: If $F_1(v) = F_2(v) = 0$, then A cannot be determined by (26).

Case 2: If $F_1(v) = 0$ and $F_2(v) \neq 0$, then $A \to \infty$.

Case 3: If $F_1(v) \neq 0$, then we have

$$A = \frac{F_2(v)}{F_1(v)}. \tag{29}$$

By varying v from 0 to 2, the curve of function $F_1(v)$ can be traced to find all zeros. Then, the curve of function A can be plotted by (29) with respect to $v \in (0,2)$ and $F_1(v) \neq 0$. From this curve, we can find the value of v corresponding to the specified A.

Remark 3: Theorem 3 can be utilized to determine whether a group of frequency-domain specifications is achievable for solving (9)-(12). As previously stated, the values of ω_{gc}, ω_{pc}, and ϕ_m that allow functions $F_1(v)$ and $F_2(v)$ to have the same zeros are inappropriate. If $F_1(v) \neq 0$ holds over the whole interval $v \in (0,\ 2)$, the value of A must be selected within the upper and lower bounds determined by (29).

3.3. The proposed design method

The design process of the FOPID controller (7) can be summarized as follows:

1) Specify the values of ω_{gc}, ω_{pc}, and ϕ_m.
2) Plot the curve of A with respect to v using (29).
3) Specify the value of A, and obtain the corresponding v value from the curve.
4) Calculate k_p, k_i and k_d using (16), (17) and (28), respectively.

The main difficulty with this method is selecting appropriate values for ω_{gc}, ω_{pc}, ϕ_m and A. These frequency-domain specifications have a direct impact on the stability, robustness and time-domain performance of the system. Generally, the magnitudes of ω_{gc} and ω_{pc} affect the rising and setting time in the response, while ϕ_m and A are related to the stability and robustness. These values can be flexibly selected according to different design requirements.

To fully clarify the distinctive contribution of this study, the proposed method can be compared to other published approaches in the following three aspects:

First, most existing approaches for tuning FOPID controllers use only the gain crossover frequency and phase margin as frequency-domain specifications. The designed controllers may lack in robustness. In our method, we consider the gain crossover frequency, phase margin, phase crossover frequency, and gain margin to improve robustness.

Second, the computation equations for the FOPID controller parameters that satisfy the frequency-domain specifications are provided in our method. By using these equations, the computational burden in the design of the FOPID controller can be significantly reduced.

Finally, the proposed method is graphical and analytical, which clearly distinguishes it from existing methods. For example, tuning methods in [23,24] were based on nonlinear optimization, and some optimization tools were required to work with nonlinear constraints. In comparison, no complex mathematical calculations are used throughout the proposed design steps. The fractional order v can be obtained intuitively in a graphical manner, while parameters k_p, k_i and k_d can be calculated directly by explicit formulas.

4. SIMULATION EXAMPLES

In this section, two fractional-order systems with time delays are presented to verify the proposed design method.

Example 1: Consider heat flow equipment modeled as the following fractional-order plus time-delay system [29]

$$P_1(s) = \frac{66.16e^{-1.93s}}{12.72s^{0.5}+1}. \tag{30}$$

The desired values of the gain crossover frequency, phase crossover frequency, and phase margin are $\omega_{gc} = 0.2$, $\omega_{pc} = 1$, and $\phi_m = 65°$, respectively. Based on these specifications, the curve of A with respect to v can be traced, as shown in Fig. 3. Suppose that the desired gain margin is $A = 5$; then, the corresponding value of v can be directly obtained from Fig. 3 as 0.7632. Thus, the proposed

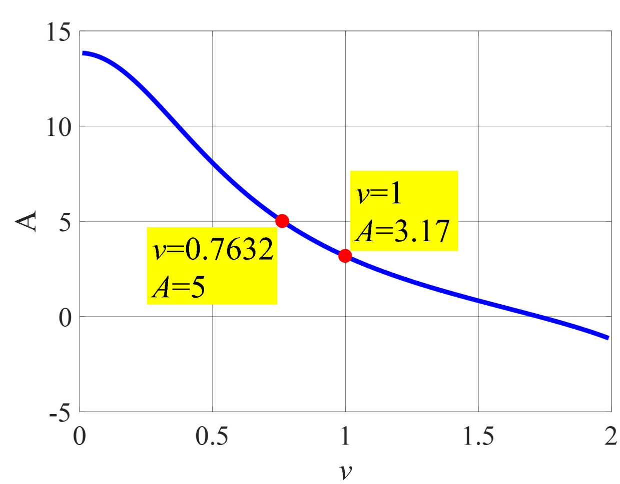

Fig. 3. The curve of A with respect to v for Example 1.

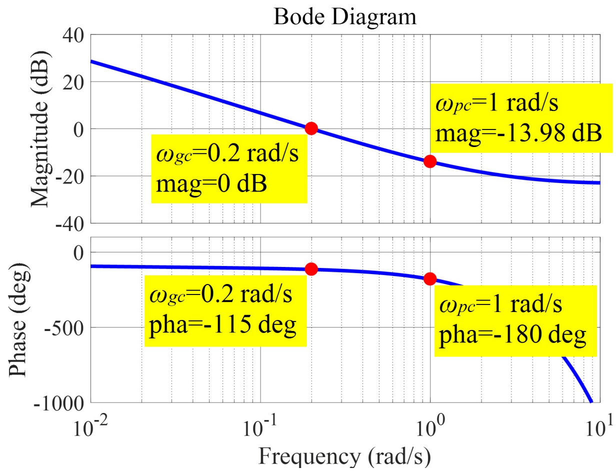

Fig. 4. Bode diagram of the open-loop system P_1C_1.

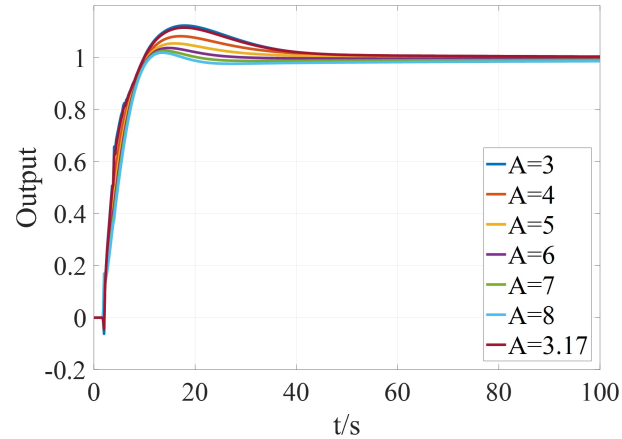

Fig. 5. Step responses of the closed-loop systems for different values of A.

Table 1. FOPID controllers for different values of A.

A	k_p	k_i	k_d	v
3	0.05998	0.0145	-0.01673	1.027
3.17	0.0569	0.0152	-0.01434	1
4	0.04239	0.01917	-0.00465	0.8809
5	0.02504	0.02523	0.005127	0.7632
6	0.005965	0.03302	0.01498	0.6652
7	-0.01682	0.04325	0.02633	0.5806
8	-0.04598	0.05706	0.04065	0.5052

FOPID controller is

$$C_1 = 0.02504 + \frac{0.02523}{s^{0.7632}} + 0.005127s^{0.7632}. \tag{31}$$

The Bode diagram of the open-loop system using controller C_1 is depicted in Fig. 4; all frequency-domain specifications are fulfilled.

By changing the value of A, different FOPID controllers can be obtained, as listed in Table 1. Specifically, the PID controller can be obtained by letting $A = 3.17$. Fig. 5 shows the step responses of the closed-loop system using these controllers. When A increases, the overshoot of the response decreases. However, the static error will increase if A is excessively large.

For $\omega_{gc} = 0.2$ and $\phi_m = 65°$, the FOPI controller designed by the method in [29] is

$$C_2 = 0.05356 + \frac{0.01649}{s^{0.973}}, \tag{32}$$

and the FOPID controller produced by the approach in [23] is

$$C_3 = -10 + \frac{0.06776}{s^{0.5831}} + 10.0115s^{0.003741}. \tag{33}$$

The step responses of the closed-loop systems using controllers C_1, C_2, and C_3 are illustrated in Fig. 6. Clearly, controller C_1 provides the lowest overshoot.

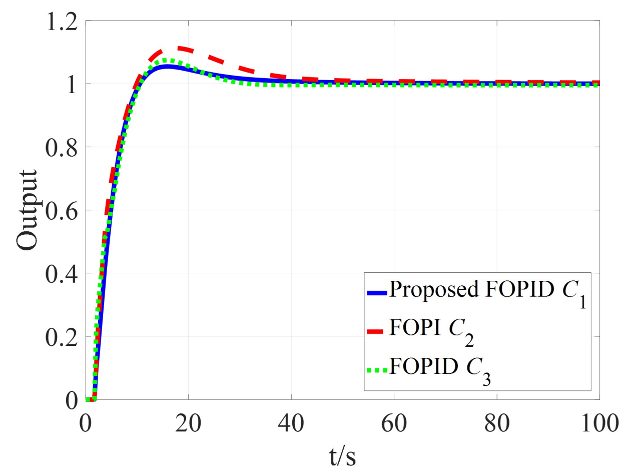

Fig. 6. Step responses of the closed-loop systems using controllers C_1, C_2 and C_3.

To test the robustness, consider that the gain K of plant P_1 varies from 16.54 to 264.64. The step responses of the closed-loop systems using different controllers for $K = 16.54$ and $K = 264.64$ are shown in Figs. 7 and 8, respectively. When $K = 16.54$, the three controllers can stabilize the control system. However, only the system with C_1 remains stable for $K = 264.64$. These results demonstrate that the proposed FOPID controller has better robustness.

Example 2: Consider a one-degree-of-freedom helicopter described by a poorly damped fractional-order model with time delay [37]

$$P_2(s) = \frac{4.2313e^{-0.6s}}{0.2s^{2.3208} + 0.41683s^{0.96} + 1}. \tag{34}$$

The required frequency-domain specifications are $\omega_{gc} = 0.4$, $\omega_{pc} = 2$, and $\phi_m = 65°$. The curve of A with respect to v is plotted in Fig. 9, which shows that the value of A tends toward infinity as v approaches 1.033. To ensure $A > 0$, the value of v must be greater than 1.033. Thus,

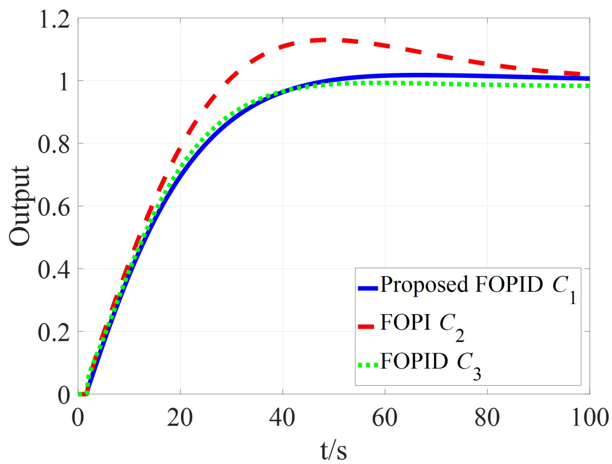

Fig. 7. Step responses of the closed-loop systems with $K = 16.54$.

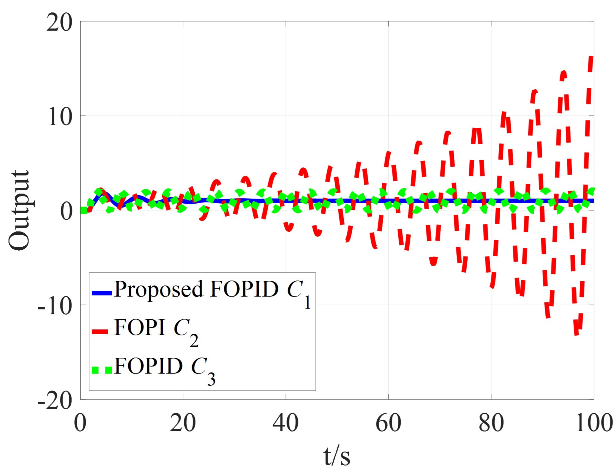

Fig. 8. Step responses of the closed-loop systems with $K = 264.64$.

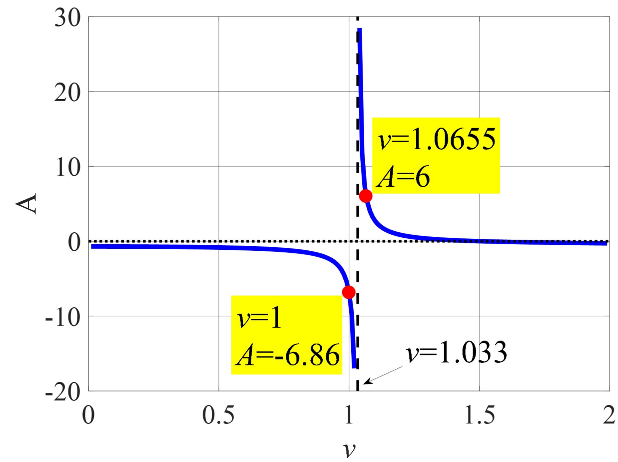

Fig. 9. The curve of A with respect to v for Example 2.

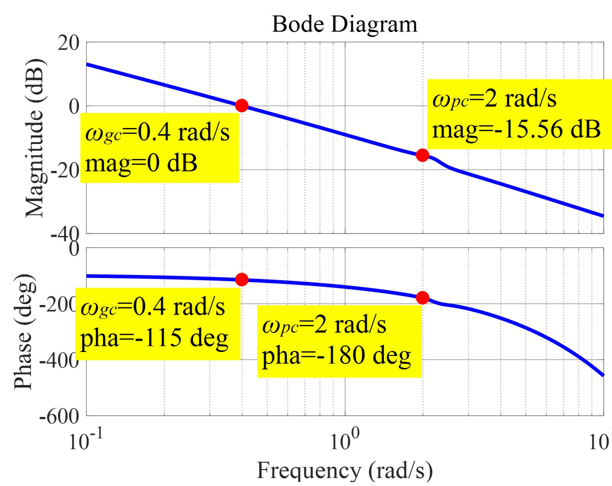

Fig. 10. Bode diagram of the open-loop system P_2C_4.

we cannot obtain a PID controller under the given specifications. Assuming that the value of A is 6, the order v is 1.0655, and the FOPID controller is designed as

$$C_4 = 0.01737 + \frac{0.09193}{s^{1.0655}} + 0.01565s^{1.0655}. \tag{35}$$

The Bode diagram of the open-loop system $P_2(s)C_4(s)$ is shown in Fig. 10: the designated ω_{gc}, ω_{pc}, ϕ_m and A are satisfied.

For $\omega_{gc} = 0.4$, $\omega_{pc} = 2$, and $A = 6$, the FOPID controllers for different values of ϕ_m are presented in Table 2. Fig. 11 illustrates the step responses of the systems with these controllers. The overshoot can be reduced by increasing the phase margin.

For a fair comparison, we set $\omega_{gc} = 0.4$ and $\phi_m = 65°$; then, the FOPI controller determined by the method in [37] is

$$C_5 = 0.07476 + \frac{0.08248}{s^{1.2147}}, \tag{36}$$

the FOPID designed by the method in [35] is

$$C_6 = 0.07916 + \frac{0.08446}{s^{1.2155}} + 0.01855s^{1.2155}, \tag{37}$$

and the FOPID tuned by the method in [23] is

$$C_7 = 0.02525 + \frac{0.08289}{s^{1.0888}} - 0.03294s^{0.8989}. \tag{38}$$

Fig. 12 compares the step responses for the systems with controllers C_4, C_5, C_6, and C_7. The proposed controller C_4

Table 2. FOPID controllers for different values of φ_m.

φ_m	k_p	k_i	k_d	v
35°	0.03278	0.06962	0.004431	1.422
45°	0.03236	0.07547	0.00709	1.3163
55°	0.02799	0.08237	0.01053	1.1995
65°	0.01737	0.09193	0.01565	1.0655
75°	-0.00645	0.1086	0.02505	0.9029
85°	-0.07305	0.1507	0.05032	0.6866

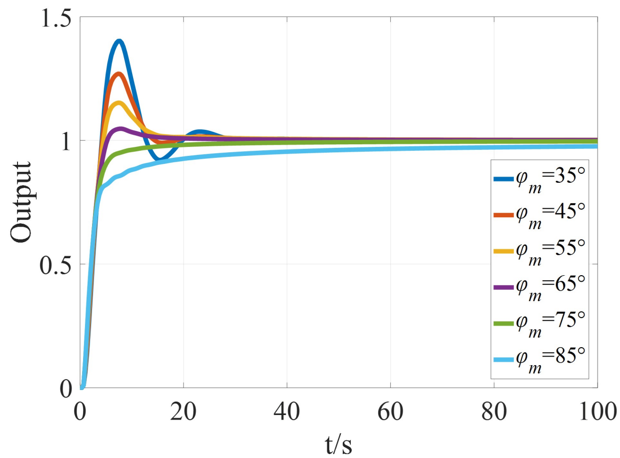

Fig. 11. Step responses of the closed-loop systems for different φ_m.

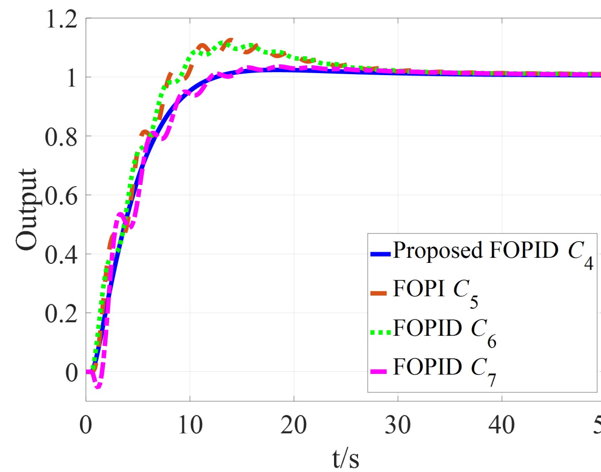

Fig. 13. Step responses of the closed-loop systems with $K = 2.11565$.

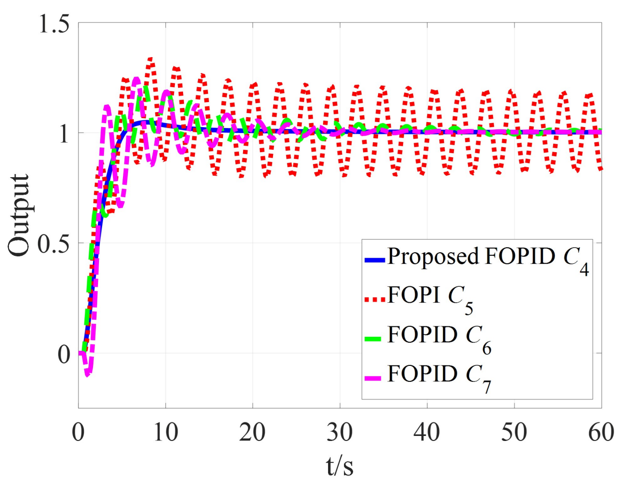

Fig. 12. Step responses of the closed-loop systems using controllers C_4, C_5, C_6, and C_7.

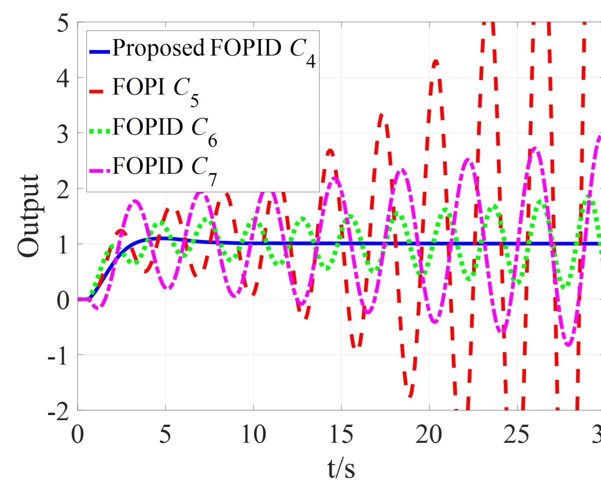

Fig. 14. Step responses of the closed-loop systems with $K = 6.34695$.

shows significant advantages in terms of overshoot, settling time and oscillation. In contrast, the control performance of C_5, C_6, and C_7 is unacceptable. In fact, the system with C_5 is nearly unstable.

To further investigate the robustness, Figs. 13 and 14 show the step responses of the systems using C_4, C_5, C_6, and C_7 when $\pm 50\%$ gain variations occur in plant P_2. C_4 is much more robust than C_5, C_6, and C_7. This result can be explained as follows. The gain margins of the systems with C_5, C_6, and C_7 are only 1.02, 1.28, and 1.4, respectively, compared with that of the system with C_4, which is 6. Excessively small gain margins result in the poor robustness of C_5, C_6, and C_7.

5. CONCLUSION

In this paper, an effective design method is proposed to simplify the tuning of FOPID controller parameters. The gain crossover frequency, phase margin, phase crossover frequency and gain margin are simultaneously utilized to establish the frequency-domain constraints. Explicit equations for directly calculating the controller parameters are formulated to replace the implicit constraints. Aided by the analytical results, the function of the gain margin with respect to the order of the FOPID controller is derived, and a graphical method is utilized to address this function. Then, the controller parameters can easily be obtained. The effectiveness of the proposed method is verified via simulation. The results show that the required frequency-domain properties are fully satisfied and that the designed FOPID controllers provide satisfactory control performance. Comparisons illustrate that the proposed

FOPID controllers provide improved robustness and time-domain performance.

In future research, we will attempt to broaden the application of the proposed method to more general systems. Because the transfer functions of these systems are more complex, obtaining the computation formulas for the controller parameters is difficult. Another interesting research topic is to extend this method to design other fractional-order controllers, such as FOPI, FOPD, and general FOPID controllers. Obviously, this method can be directly applied to the design of three-parameter FOPI and FOPD controllers. However, additional design criteria are required for the FOPID controller with five adjustable parameters.

REFERENCES

[1] A. Maachou, R. Malti, P. Melchior, J.-L. Battaglia, and B. Hay, "Thermal system identification using fractional models for high temperature levels around different operating points," *Nonlinear Dynamics*, vol. 70, no. 2, pp. 941-950, October 2012.

[2] S. Luo, F. L. Lewis, Y. Song, and K. G. Vamvoudakis, "Adaptive backstepping optimal control of a fractional-order chaotic magnetic-field electromechanical transducer," *Nonlinear Dynamics*, vol. 100, no. 1, pp. 523-540, March 2020.

[3] E. Loghman, A. Kamali, F. Bakhtiari-Nejad, and M. Abbaszadeh, "Nonlinear free and forced vibrations of fractional modeled viscoelastic FGM micro-beam," *Applied Mathematical Modelling*, vol. 92, pp. 297-314, April 2021.

[4] J. Shi, J. Zheng, X. Liu, W. Xiang, and Q. Zhang, "Novel short-time fractional Fourier transform: Theory, implementation, and applications," *IEEE Transactions on Signal Processing*, vol. 68, pp. 3280-3295, May 2020.

[5] Y. Wang, H. Zhong, and B. Wang, "Fractional order model of three-winding series-connected single-phase motor," *Proc. of 20th International Conference on Electrical Machines and Systems (ICEMS)*, pp. 1-4, October 2017.

[6] P. Liu, Z. Zeng, and J. Wang, "Asymptotic and finite-time cluster synchronization of coupled fractional-order neural networks with time delay," *IEEE Transactions on Neural Networks and Learning Systems*, vol. 31, no. 11, pp. 4956-4967, January 2020.

[7] P. Chen, B. Wang, Y. Tian, and Y. Yang, "Finite-time stability of a time-delay fractional-order hydraulic turbine regulating system," *IEEE Access*, vol. 7, pp. 82613-82623, June 2019.

[8] L. Bai and D. Xue, "Universal block diagram based modeling and simulation schemes for fractional-order control systems," *ISA Transactions*, vol. 82, pp. 153-162, November 2018.

[9] D. Li, L. Wei, T. Song, and Q. Jin, "Study on asymptotic stability of fractional singular systems with time delay," *International Journal of Control, Automation, and Systems*, vol. 18, no. 4, pp. 1002-1011, April 2020.

[10] D. Li, X. He, T. Song, and Q. Jin, "Fractional order IMC controller design for two-input-two-output fractional order system," *International Journal of Control, Automation, and Systems*, vol. 17, no. 4, pp. 936-947, April 2019.

[11] V. Feliu-Batlle, R. Rivas-Perez, and F. J. Castillo-García, "Simple fractional order controller combined with a Smith predictor for temperature control in a steel slab reheating furnace," *International Journal of Control, Automation, and Systems*, vol. 11, no. 3, pp. 533-544, June 2013.

[12] P. P. Arya and S. Chakrabarty, "A robust internal model-based fractional order controller for fractional order plus time delay processes," *IEEE Control Systems Letters*, vol. 4, no. 4, pp. 862-867, May 2020.

[13] C. Ding, J. Cao, and Y. Chen, "Fractional-order model and experimental verification for broadband hysteresis in piezoelectric actuators," *Nonlinear Dynamics*, vol. 98, no. 4, pp. 3143-3153, December 2019.

[14] A. Jalloul, J.-C. Trigeassou, K. Jelassi, and P. Melchior, "Fractional order modeling of rotor skin effect in induction machines," *Nonlinear Dynamics*, vol. 73, no. 1, pp. 801-813, July 2013.

[15] M. Sharma, B. S. Rajpurohit, S. Agnihotri, and A. K. Rathore, "Development of fractional order modeling of voltage source converters," *IEEE Access*, vol. 8, pp. 131750-131759, July 2020.

[16] J. Xu, X. Li, X. Meng, J. Qin, and H. Liu, "Modeling and analysis of a single-phase fractional-order voltage source pulse width modulation rectifier," *Journal of Power Sources*, vol. 479, p. 228821, December 2020.

[17] S. Kumar and A. Ghosh, "An improved fractional-order circuit model for voltammetric taste sensor system with infused tea as analyte," *IEEE Sensors Journal*, vol. 20, no. 14, pp. 7792-7800, March 2020.

[18] B. Hekimoğlu, "Optimal tuning of fractional order PID controller for DC motor speed control via chaotic atom search optimization algorithm," *IEEE Access*, vol. 7, pp. 38100-38114, March 2019.

[19] R. K. Jatoth, V. Kishore K, N. Bhookya, and G. Ramesh, "A comparative study on design and tuning of integer and fractional order PID controller," *Proc. of 2014 International Conference on Modelling, Identification & Control*, pp. 160-165, December 2014.

[20] X. Li, Y. Wang, N. Li, M. Han, Y. Tang, and F. Liu, "Optimal fractional order PID controller design for automatic voltage regulator system based on reference model using particle swarm optimization," *International Journal of Machine Learning and Cybernetics*, vol. 8, no. 5, pp. 1595-1605, October 2017.

[21] F. Martín, C. A. Monje, L. Moreno, and C. Balaguer, "DE-based tuning of $PI^{\lambda}D^{\mu}$ controllers," *ISA Transactions*, vol. 59, pp. 398-407, November 2015.

[22] A. Asgharnia, A. Jamali, R. Shahnazi, and A. Maheri, "Load mitigation of a class of 5-MW wind turbine with RBF neural network based fractional-order PID controller," *ISA Transactions*, vol. 96, pp. 272-286, January 2020.

[23] C. A. Monje, B. M. Vinagre, V. Feliu, and Y. Chen, "Tuning and auto-tuning of fractional order controllers for industry applications," *Control Engineering Practice*, vol. 16, no. 7, pp. 798-812, July 2008.

[24] F. Meng, S. Liu, A. Pang, and K. Liu, "Fractional order PID parameter tuning for solar collector system based on frequency domain analysis," *IEEE Access*, vol. 8, pp. 148980-148988, August 2020.

[25] S. Das, S. Saha, S. Das, and A. Gupta, "On the selection of tuning methodology of FOPID controllers for the control of higher order processes," *ISA Transactions*, vol. 50, no. 3, pp. 376-388, July 2011.

[26] X. Li and L. Gao, "Robust fractional-order PID tuning method for a plant with an uncertain parameter," *International Journal of Control, Automation, and Systems*, vol. 19, no. 3, pp. 1302-1310, March 2021.

[27] E. Yumuk, M. Güzelkaya, and İ. Eksin, "Analytical fractional PID controller design based on Bode's ideal transfer function plus time delay," *ISA Transactions*, vol. 91, pp. 196-206, August 2019.

[28] Z.-Y. Nie, Y.-M. Zheng, Q.-G. Wang, R.-J. Liu, and L.-J. Xiang, "Fractional-order PID controller design for time-delay systems based on modified Bode's ideal transfer function," *IEEE Access*, vol. 8, pp. 103500-103510, May 2020.

[29] H. Malek, Y. Luo, and Y. Chen, "Identification and tuning fractional order proportional integral controllers for time delayed systems with a fractional pole," *Mechatronics*, vol. 23, no. 7, pp. 746-754, October 2013.

[30] V. Feliu-Batlle and R. Rivas-Perez, "Robust fractional-order controller for an EAF electrode position system," *Control Engineering Practice*, vol. 56, pp. 159-173, November 2016.

[31] C. A. Monje, A. J. Calderon, B. M. Vinagre, Y. Chen, and V. Feliu, "On fractional PI^{λ} controllers: Some tuning rules for robustness to plant uncertainties," *Nonlinear Dynamics*, vol. 38, no. 1, pp. 369-381, December 2004.

[32] C. I. Muresan, S. Folea, I. R. Birs, and C. Ionescu, "A novel fractional-order model and controller for vibration suppression in flexible smart beam," *Nonlinear Dynamics*, vol. 93, no. 2, pp. 525-541, July 2018.

[33] S. P. Nangrani and S. S. Bhat, "Fractional order controller for controlling power system dynamic behavior," *Asian Journal of Control*, vol. 20, no. 1, pp. 403-414, January 2018.

[34] W. Zheng, Y. Luo, Y. Pi, and Y. Chen, "An improved frequency-domain design method for the fractional order PID controller optimal design: A case study of permanent magnet synchronous motor speed control," *IET Control Theory and Applications*, vol. 12, no. 18, pp. 2478-2487, December 2018.

[35] A. Chevalier, C. Francis, C. Copot, C. M. Ionescu, and R. De Keyser, "Fractional-order PID design: Towards transition from state-of-art to state-of-use," *ISA Transactions*, vol. 84, pp. 178-186, January 2019.

[36] S. P. Jadhav, R. H. Chile, and S. T. Hamde, "A simple method to design robust fractional-order lead compensator," *International Journal of Control, Automation, and Systems*, vol. 15, no. 3, pp. 1236-1248, June 2017.

[37] I. Birs, C. Muresan, D. Copot, I. Nascu, and C. Ionescu, "Design and practical implementation of a fractional order proportional integral controller (FOPI) for a poorly damped fractional order process with time delay," *Proc. of 7th International Conference on Control, Mechatronics and Automation (ICCMA)*, pp. 56-61, November 2019.

Xu Li received his M.S. degree from the Hefei University of Technology, Hefei, China, in 2014. He is currently pursuing a Ph.D. degree in the Department of Automation, University of Science and Technology of China, Hefei, China. His research interests include fractional order systems, nonlinear systems, nonlinear control, and industrial process control.

Lifu Gao received his M.S. degree in pattern recognition and intelligent systems from the Institute of Intelligent Machines, Chinese Academy of Sciences, Hefei, China, in 1999 and a Ph.D. degree in pattern recognition and intelligent systems from the University of Science and Technology of China, Hefei, China, in 2002. From 2005 to 2011, he was a postdoctoral fellow and a senior engineer with European Molecular Biology Laboratory, Hamburg, Germany. Since 2011, he has been a research fellow with the Institute of Intelligent Machines, Chinese Academy of Sciences, Hefei, China. His research interests include robotics and sensors.